Hindawi
Advances in Civil Engineering
Volume 2022, Article ID 1963553, 19 pages
https://doi.org/10.1155/2022/1963553

Research Article

Scaling Method Application for Seismic Design along the Central Anatolian Fault Zone

Erhan Gumus,[1] **Baki Ozturk**,[2] **and Fadzli Mohamed Nazri**[3]

[1]*Department of Risky Structures, Directorate General for Infrastructure and Urban Transformation Services, Ministry of Environment, Urbanization and Climate Change, Ankara 06510, Turkey*
[2]*Department of Civil Engineering, Hacettepe University, Ankara 06800, Turkey*
[3]*School of Civil Engineering, Universiti Sains Malaysia, Engineering Campus, Nibong Tebal, Penang, Malaysia*

Correspondence should be addressed to Baki Ozturk; bakiozturk@hacettepe.edu.tr

Received 18 April 2022; Accepted 27 July 2022; Published 27 August 2022

Academic Editor: Dawei Yin

Cities located along the Central Anatolian Fault Zone (CAFZ), such as Kayseri and Mersin, have become metropolitan cities in Turkey since the 1950s and have been attracting big investments, such as the Akkuyu Nuclear Power Plant (Mersin), which is planned to be built close to the CAFZ. In this study, the ground motion records of earthquakes occurring along the CAFZ are scaled for single-degree-of-freedom (SDOF) systems conforming to the current design response spectra. This is a pioneering study on the analysis of seismic behavior using SDOF systems subjected to ground motions that were recorded in relation to earthquakes occurring on the CAFZ in Turkey. It defines the importance of selecting suitable records with certain features that can be used with the scaling method to ensure that real ground motion records match the design acceleration spectra defined in the earthquake codes and will provide a perspective on future destructive earthquakes that may occur on the CAFZ.

1. Introduction

Time domain analysis is frequently used to determine specifications involved in the design of structures regarding their earthquake performance. Acceleration records are required for such analyses if they are compatible with design spectra obtained from synthetic, simulated, or real earthquake records [1–3].

Real acceleration records obtained from earthquakes are more easily accessible nowadays, and thus, the use of real ground motion records is preferable for use in analysis. However, a large amount of different data pertaining to various parameters often exists, such as earthquake magnitude, scaled acceleration records, fault type, local ground conditions of stations, and distance from the earthquake source, and thus, it is difficult to obtain records specific to the actual situation in some cases [4]. Therefore, real earthquake records that fulfill conditions set out in earthquake codes are required, and these need to be scaled by adjusting with design response spectrum [5].

A large number of studies have been conducted [6] involving the selection and scaling of related codes using records obtained from real earthquakes, with the aim of using such information in structural design. These studies have analyzed methods used in the selection and scaling of records obtained from real earthquakes occurring in countries, such as the United States of America, China, European Union countries, New Zealand, and Taiwan, and reveal differences and similarities between the codes applied [5, 7–17]. In addition, studies have been conducted to select and scale earthquake records in the time domain.

Scholz [18] addressed the problem of how to predict strong ground motions for very large earthquakes from observations made of such motions produced by events of moderate size. McGarr [19] described how the state of stress as well as the focal depth clearly is an important factor to be considered in the prediction of seismic ground motion. Somerville [20] reviewed the magnitude scaling of near-fault ground motions. Kurama and Farrow [21] showed that scaling methods that work well for ground motions

representative of stiff soil and far-field conditions lose their effectiveness for soft soil and near-field conditions for a wide range of structural characteristics. Naeim et al. [22] presented a new approach to the selection and scaling of ground motion time histories for structural design using genetic algorithms. Watson-Lamprey and Abrahamson [23] proposed a procedure to select time series for use in nonlinear analyses that is intended to result in an average response of the nonlinear system that is not based simply on magnitude, distance, and spectral shape. Luco and Bazzurro [24] demonstrated that scaling can indeed introduce a bias that, for the most part, can be explained by differences between the elastic response spectra of the scaled and unscaled records. Kottke and Rathje [25] defined a semiautomated procedure for selecting and scaling recorded earthquake motions for dynamic analysis. Huang et al. [26] proposed a scaling method that explicitly considers spectral shape. Katsanos et al. [27] reviewed alternative selection procedures based on established methods for incorporating strong ground motion records within the framework of seismic design of structures. Jayaram et al. [28] defined a computationally efficient ground-motion selection algorithm for matching a target response spectrum mean and variance. Takewaki and Tsujimoto [29] defined the scaling of design earthquake ground motions for tall buildings based on drift and input energy demands. Ay and Akkar [30] presented a ground-motion selection and scaling methodology that preserves the basic seismological features of the scaled records with reduced scatter in the nonlinear structural response. Haselton et al. [31] provided guidance to design professionals on the selection and scaling of ground motions for the purpose of nonlinear response history analysis. Al Atik et al. [32] described a method for deriving kappa (κ) scaling factors that can be applied to ground motion prediction equations (GMPEs) to account for site-specific κ estimates.

Historically, in 1717 [33] and 1835 [34], two major destructive earthquakes occurred at the Central Anatolian Fault Zone (CAFZ). In the 20th century, two subsequent destructive earthquakes occurred in 1940 along the CAFZ. In January, an earthquake of $M_s = 5.0$ magnitude occurred, during which 58 people lost their lives, while in February, an earthquake of $M_s = 6.7$ magnitude occurred, during which 37 people lost their lives [34].

Since the 1950s there has been significant urbanization in Turkey, accompanied by a rapid increase in the population of big cities. Cities located along the CAFZ, such as Kayseri and Mersin, have become metropolitan cities in Anatolia due to the high increase in population of Turkey during this era. Mersin (approximately 1.7 million people) and Kayseri (approximately 1.4 million people) are attracting big investments, such as the Akkuyu Nuclear Power Plant (Mersin), which is planned to be built close to the CAFZ.

However, to date, no study has been conducted on the scaling of records of real earthquakes that have occurred on the CAFZ in Middle Anatolia, Turkey, for use either in structural design or in the assessment of the earthquake performance of existing structures. This study is therefore the first to consider the ground motion records of earthquakes occurring on the CAFZ in terms of the analysis of the seismic behavior of single-degree-of-freedom (SDOF) systems. In this respect, this study provides results that can be used in implementing earthquake engineering performance-based design principles within this seismic area.

In this study, general methods and criteria that are used to select earthquake records are discussed, and the records of earthquakes that occurred on the CAFZ are scaled to conform to the design response spectra of [35]. In addition, for SDOF linear systems with a 5% damping ratio and response spectra in the period from $T_S = 0.01$ to $T_F = 2.00$ s, spectral relative response, spectral velocity, and spectral displacement form are calculated. This research is being conducted between $T_S = 0.01$ s and $T_F = 2.00$ s since this period range covers the seismic design periods of almost all the building structures located along the CAFZ. It should be noted that this study will provide a perspective on future destructive earthquakes that may occur on the CAFZ that will affect the new metropolitan cities of Kayseri and Mersin.

2. Records of Earthquakes Occurring in the Central Anatolian Fault Zone, Turkey

The Central Anatolian Fault Zone (CAFZ) stretches over 700 km, beginning at a point to the west of the city of Mersin. It travels through the Gulek Strait, Pozanti, and Camardi (Nigde) to Erciyes (N20E), after which it changes direction (N50E) in the direction of Gemerek, Sarkisla, and Sivas. It eventually reaches the North Anatolian fault zone at Erzincan [36, 37], making it the second largest fault zone in Anatolia after the North Anatolian fault zone. A simplified map showing the neotectonic subdivision of Turkey and adjacent areas [38] is shown in Figure 1, while a simplified map showing major structural elements of east Central Anatolia [39] is provided in Figure 2.

The records of earthquakes occurring on the CAFZ are supplied by the Strong Ground Motion Database of Turkey. Figure 3 shows the 17 ground motion records selected for this study from earthquakes that occurred between 1976 and 2014 with a magnitude of $M \geq 2.8$. Further details of these earthquakes are supplied in Table 1, which shows the associated station location, ground conditions, distance, magnitude, acceleration values, and scaling factors related to these records.

3. Selection and Scaling of Real Earthquake Records in Line with the Design Response Spectra

The calculations of the seismic load on structures can be conducted using the "*Equivalent Static Earthquake Load Method*" and "*Mode Combination Method*." Recent advances in technological developments have enabled the use of nonelastic calculation methods to be used in the design of structures when performing a structural analysis in the time domain. It is thus possible to conduct research on the selection of appropriate seismic records and associated scaling of such records using either a linear elastic or nonlinear inelastic analysis in the time domain.

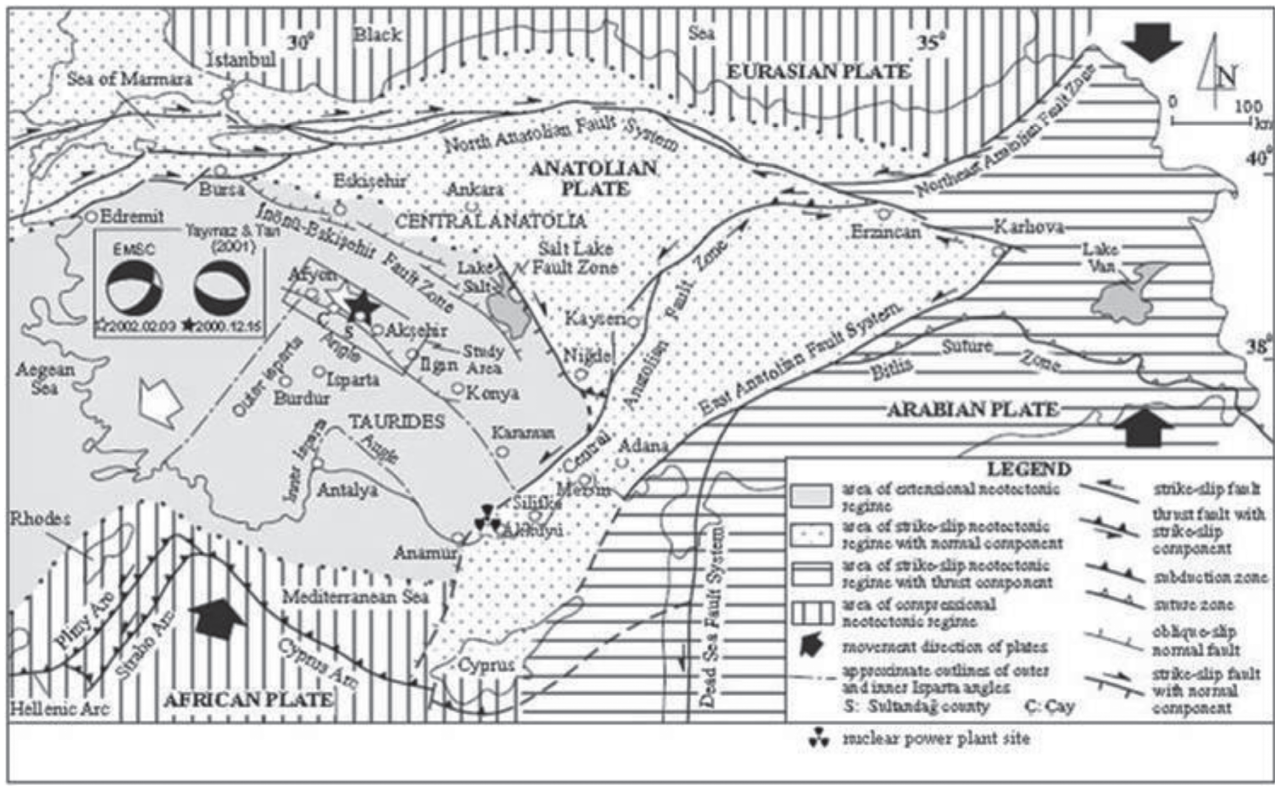

Figure 1: Simplified map showing the neotectonic subdivision of Turkey and adjacent areas [38] (location of the Akkuyu Nuclear Power Plant site is plotted on the map.).

3.1. Earthquake Record Sources. Accelerograms are used in earthquake calculations practiced in time-domain structural analysis and obtained from three different sources, which are described below [1–3].

3.1.1. Earthquake Records Generated Synthetically. Over a wide-ranging period, it is possible to generate synthetic records that are similar to those of an actual response spectrum. For example, the power spectral density function is calculated from simplified response spectra, and sinusoidal signals are generated by compounding this function with random phase angles; a synthetic record is thus obtained by collecting these sinusoidal functions. Moreover, an iterative method can be used to enhance matching with the design spectrum, wherein the scaling factor between the ordinates of a real response spectrum and a target design spectrum is calculated at a selected frequency. It is then possible to correct the record by adjusting the power spectral density function with the square of this scaling constant. As a result of these processes, new ground motion can be obtained.

3.1.2. Simulated Earthquake Records. Simulated earthquake records are obtained from seismological source models that consider the propagation medium and ground conditions. In that condition, the most different subject is the identification of suitable source, propagation medium, and ground conditions. In analyses used to obtain the physically simulated records of source and wave propagation characteristics for the area to be examined, it is necessary to identify an earthquake scenario that depends on magnitude and distance. However, this information is usually unavailable, particularly, in cases where seismic design codes are used [4].

3.1.3. Records Obtained from Real Earthquakes. Real earthquake records include accurate information about certain characteristics and the nature of ground shaking (amplitude, duration, phase characteristics, and frequency content). They also reflect factors, such as the source influencing the records, propagation medium, and ground conditions. Therefore, with respect to the seismological parameters of an area, the selection of such records is more beneficial compared with other alternatives.

3.2. Selection of Real Earthquake Records. Real earthquake records are generally selected from locations where either the design spectrum is provided to represent the specified characteristics of ground motion or the earthquake scenario is given with minimum parameters, such as magnitude distance and soil class. Records selected for a specified region should be matched with the generated response spectrum because of seismic hazard analysis and should satisfy the geological and seismological conditions.

The magnitude of an earthquake strongly influences the frequency content and duration of ground motion, and thus,

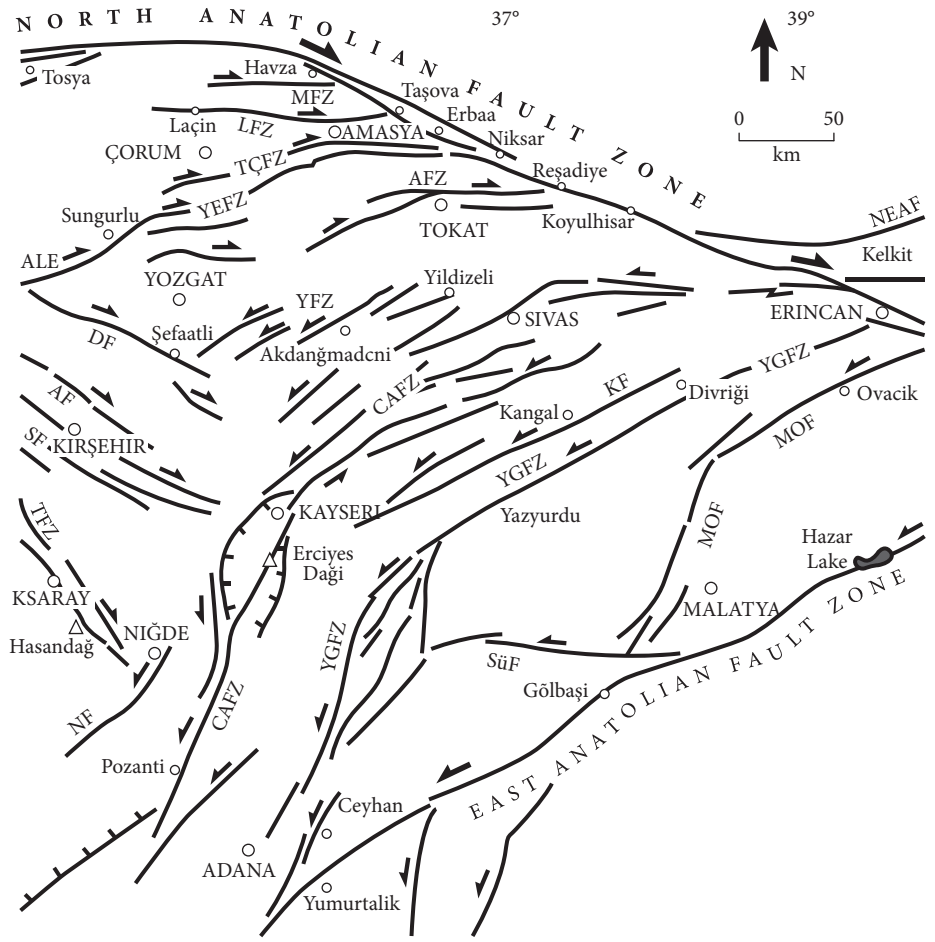

Figure 2: Simplified map showing major structural elements of east central Anatolia [39].

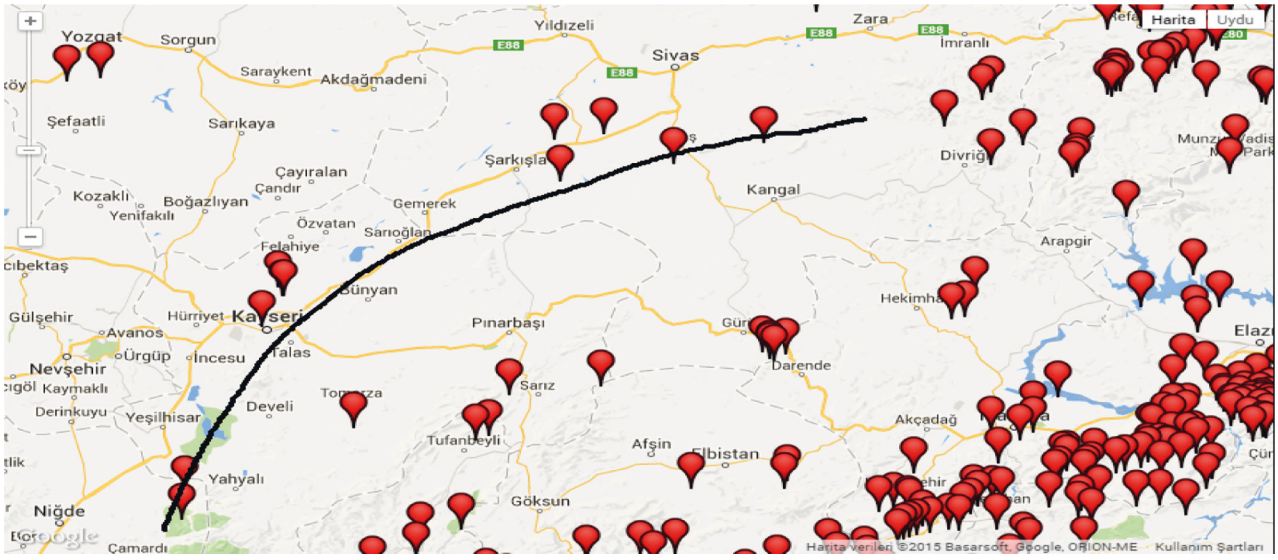

Figure 3: Earthquakes recorded on the Central Anatolian Fault Zone (CAFZ) by the strong ground motion database of Turkey [40].

it is important to select records of events with appropriate magnitudes. For example, the earthquake magnitude of selected records needs to be approximately ±0.25 of the target magnitude [41].

3.3. Ground Motion Scaling Methods. Real earthquake records can be scaled in either the frequency or time domains using scaling methods. The scaling method used in the frequency domain alters the frequency content of the

Table 1: Details and calculated scaling constant (α_{ST}) of records of earthquakes that occurred throughout the Central Anatolian Fault Zone (CAFZ), Turkey.

Station		Date	Magnitude	Soil type	Earthquake zone	Recorded max. acceleration value (gal)			North-south (N-S)		East-west (E-W)	
Province	Country					N-S	E-W	U-D	Scaling constant (α ST)	Fractional relative error (%)	Scaling constant (α ST)	Fractional relative error (%)
Tokat	Centrum	11.06.1999	4.1	Z3	1	1.9	1.1	0.64	1.4	17.28	4.9	16.25
Tokat	Centrum	11.06.1999	4.5	Z3	1	4.11	1.4	1.1	1.1	18.2	1.1	17.81
Tokat	Centrum	14.04.2006	2.8	Z3	1	10.1	5.7	12.9	1.4	1.11	7.9	1.10
Kirikkale	Centrum	12.08.2008	4.8	Z2	1	0.66	0.68	0.31	4.7	15.55	4.12	15.68
Ankara	Bala	12.08.2008	4.8	Z2	2	0.29	0.4	0.14	1.7	18.99	1.7	18.12
Ankara	S. kochisar	12.08.2008.	4.8	Z3	2	0.35	0.37	0.25	7.4	18.53	7.6	17.88
Aksaray	Centrum	12.08.2008	4.8	Z3	5	0.59	0.77	0.29	3.4	22.8	1.2	22.83
Kayseri	Centrum	13.11.2008	3.7	Z2	3	0.35	0.33	0.36	1.9	20.23	1.9	19.9
Kayseri	Centrum	19.11.2008	3.6	Z2	3	0.62	0.7	0.45	1.9	20.79	1.10	20.79
Kayseri	Centrum	15.01.2009	3.7–3.9	Z2	3	1.2	1.2	1.1	1.2	20.29	2.1	19.63
Nigde	Centrum	30.01.2009	4.3	Z2	4	1.3	1.2	1.8	1.1	22.9	1.1	22.46
Nevsehir	Centrum	30.09.2011	4.3	Z2	3	0.9	1.1	0.79	1.10	19.61	7.6	19.94
Sivas	Ulas	30.08.2013	3.3	Z2	4	0.34	1.01	0.47	26.13	22.29	—	—
Nigde	Camardi	01.11.2013	3.7	Z3	4	1.3	1.2	1.2	1.1	23.59	1.2	23.44
Sivas	Kangal	01.05.2014	4.2	Z2	4	0.6	0.61	0.47	1.6	23.48	1.5	23.13
Kayseri	Centrum	26.03.2015	3.8	Z2	3	0.52	0.46	0.38	8.4	20.78	1.10	20.3
Sivas	Gemerek	26./03/2015	3.8	Z2	3	0.66	0.62	0.27	12.2	19.27	1.9	20.1

accelerogram, whereas in the time domain, the amplitude of the record is changed.

3.3.1. Scaling of Ground Motion in Frequency Domain. In this method, records are generated that are compatible with the design response spectrum recorded by accelerograms. This is a more effective method than other methods of earthquake record production, as the earthquake motion does not lose its physical characteristics during scaling in the frequency domain [42]. Using a scaling method in the frequency domain, attaining records that precisely match the design spectrum is possible. However, when these records are used in the nonlinear earthquake calculations of structures, it is necessary to determine whether an equal displacement rule in the sensitive area applies [43].

3.3.2. Ground Motion Scaling in Time Domain. In this approach, the recorded ground motion is simply scaled up or down uniformly (multiplying by greater than one or less than one and by a constant) so that the results have the best match with the target spectrum within a period range of interest. When the use of more than one earthquake record is required, it is possible either to fit each record separately or to best fit the average of the produced spectra to the target spectrum.

Scaling in the time domain is based on minimizing the difference between the scaled behavior spectrum and the design response spectrum using the least-square method. The "difference" is scaled and defined as an integration of the square of differences among the target design spectrum amplitudes. It is calculated using the following equation:

Table 2: Spectrum characteristic periods, T_A and T_B.

Site class	T_A (sec)	T_B (sec)
Z1	0.10	0.30
Z2	0.15	0.40
Z3	0.15	0.60
Z4	0.20	0.90

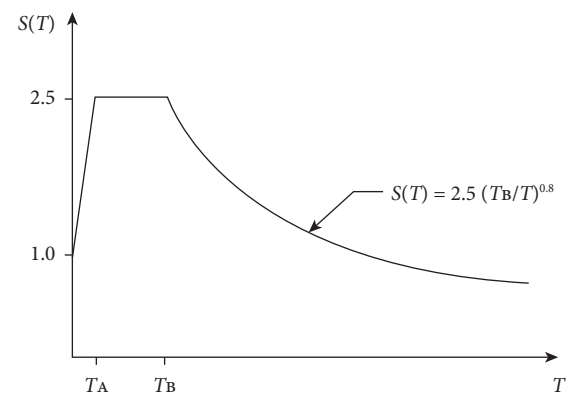

Figure 4: Spectrum function.

$$|Difference| = \int_{TS}^{TF} \left[\alpha S_a^{actual}(T) - S_a^{target}(T)\right]^2 dT, \quad (1)$$

where S_a^{target} is the target acceleration response spectrum, S_a^{actual} is the acceleration spectrum of the real earthquake record used, α is the linear scaling factor, T is the period of the oscillator, T_S is the lower period range of scaling used, and T_F is the upper period range of scaling used.

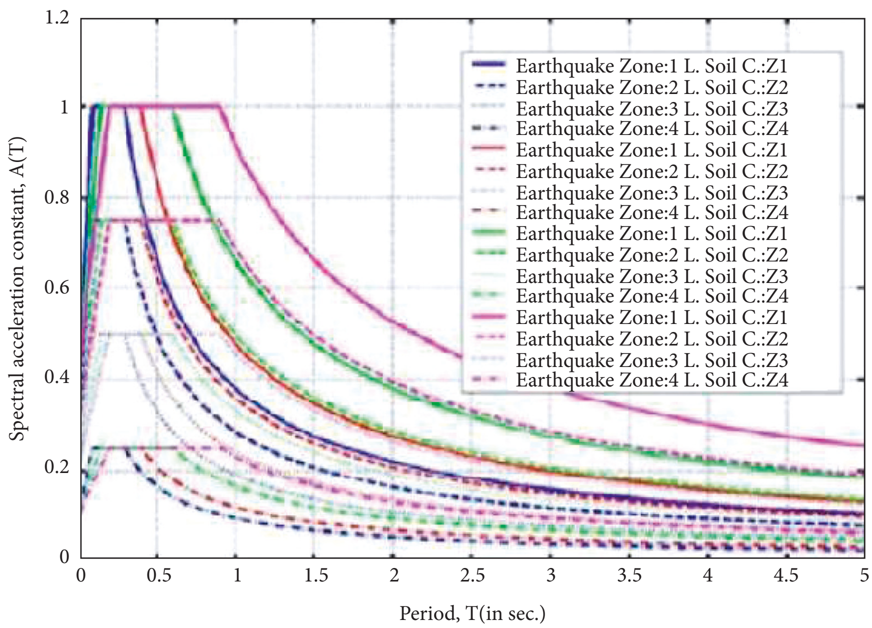

Figure 5: Elastic design acceleration spectra for four different earthquake zones and different local site classes [5].

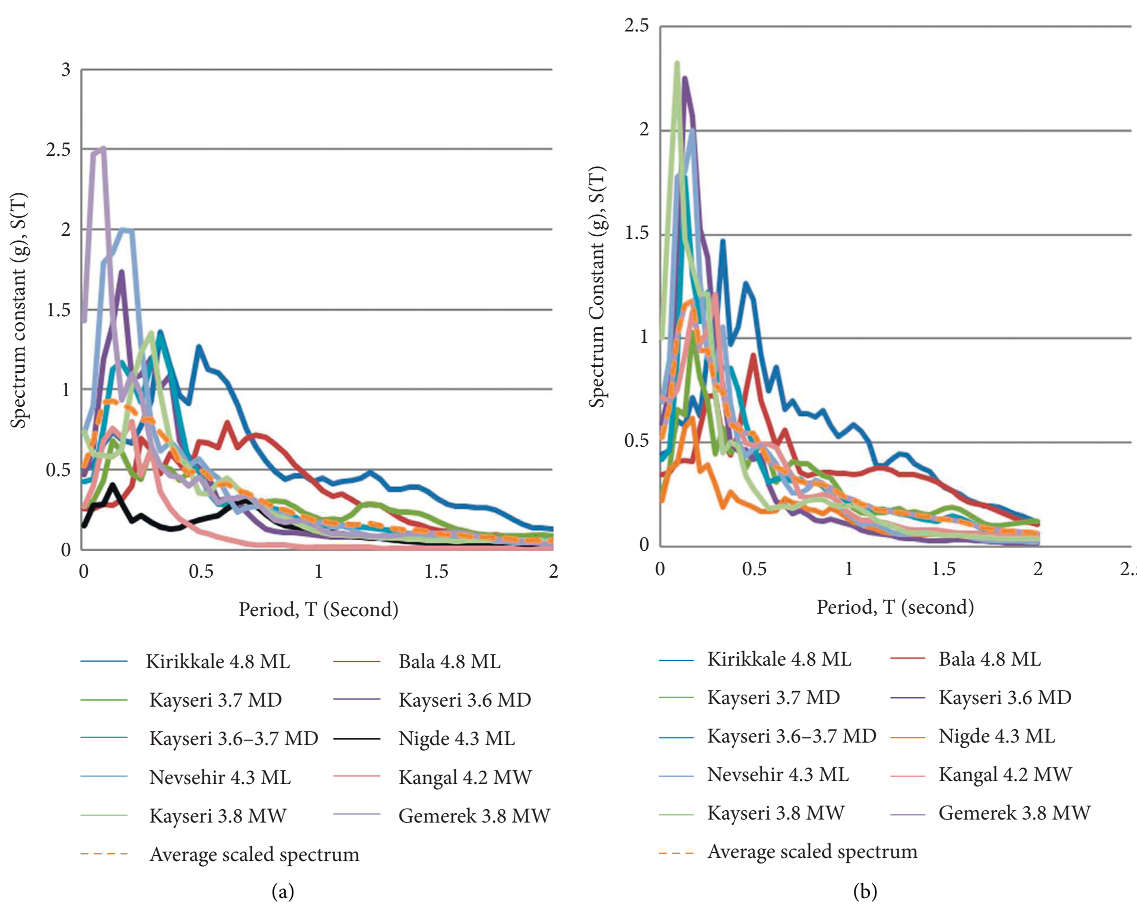

Figure 6: Response spectra of earthquake records scaled according to elastic design acceleration spectrum (with local site class Z2); (a) North-South (N-S) and (b) East-West (E-W) components.

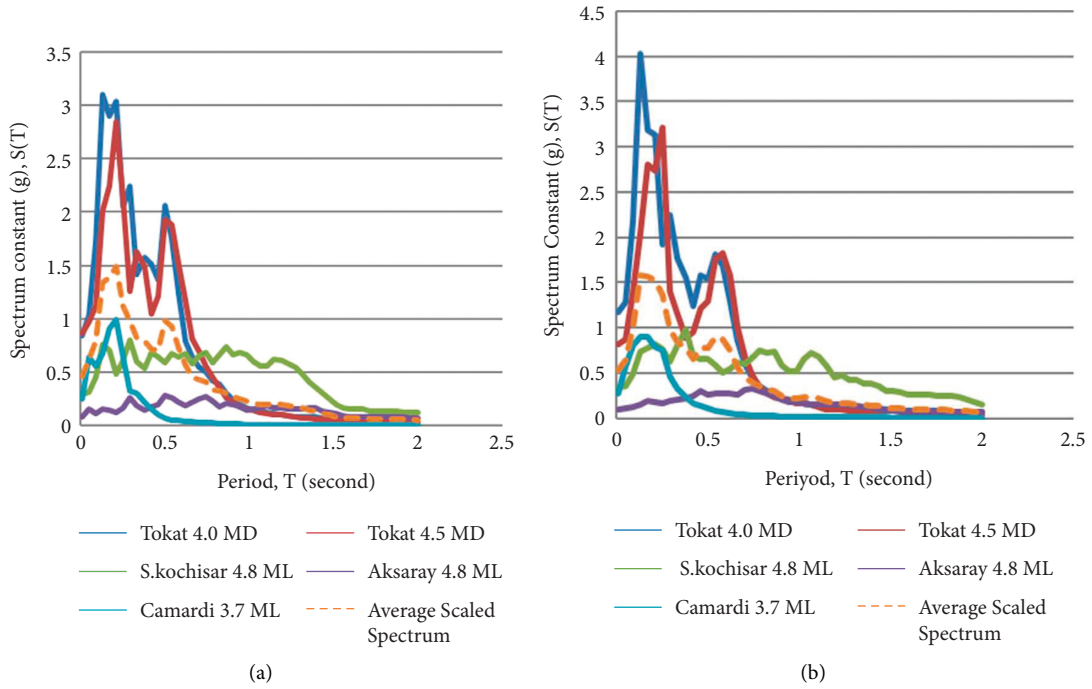

Figure 7: Response spectra of earthquake records scaled according to elastic design acceleration spectrum (with local site class Z3); (a) North-South (N-S) and (b) East-West (E-W) components.

To minimize the difference, the derivative of the "difference" function with respect to the scaling factor must be zero, as follows:

$$\min |\text{Difference}| \text{occurs at} \frac{d|\text{Difference}|}{d\alpha} = 0, \quad (2)$$

where the "difference" function in Equation (1) is equated to zero by taking a derivative with respect to $d\alpha$. By changing the integrals in Equation (1) to discrete forms, a total form continuing to T_F with a ΔT (step) increment from T_S is obtained, where ΔT is the period step increment, as in the following equation.

$$\alpha = \frac{\sum_{T=T_A}^{T_B} \left(S_a^{actual}(T) * S_a^{target}(T)\right)}{\sum_{T=T_A}^{T_B} \left(S_a^{actual}(T)\right)^2}. \quad (3)$$

3.4. Selection and Scaling of Real Records according to the Design Spectra. In the earthquake codes, the design earthquake is accepted as being a ground motion that has a 10% probability of exceedance within a period of 50 years. To show this ground motion, a spectrum constant, $S(T)$, depending on local site classes with a 5% damping ratio, is identified. The differences of the local site classes on the design spectrum are reflected with the help of spectrum characteristic periods (T_A and T_B); and [35] provides characteristic periods corresponding to four different site classes (Table 2).

The design spectrum function is given in Figure 4. The elastic spectral acceleration constant, $A(T)$, used in analysis is calculated by multiplying $S(T)$, which is equivalent to the period of the structure; the effective ground acceleration constant, A_o, which shows the earthquake risk within the region; and the building importance constant, I, which varies according to the utilization type of the buildings, as follows.

$$A(T) = A_o I S(T). \quad (4)$$

The spectrum constant, $S(T)$, is evaluated according to the following equation.

$$S(T) = 1 + 1.5\frac{T}{T_A}, \quad (0 \le T \le T_A),$$
$$S(T) = 2.5, \quad (T_A < T \le T_B), \quad (5)$$
$$S(T) = 2.5\left(\frac{T_B}{T}\right)^{0.8}, \quad (T_B < T).$$

Site classes provided are shown in Figure 5, together with the elastic spectral acceleration constants drawn for different earthquake zones. A_o is defined regarding the existing faults and records of prior earthquakes, and Turkey is separated into five earthquake zones.

3.4.1. Definition of Scaling Constant for Elastic Spectral Acceleration. $A(T)$ is obtained by multiplying A_o,I, and $S(T)$. In this study, records are selected and scaled only for $S(T)$ using this feature; the scaling constant obtained from this process is named α_{ST}. In addition, α_{AT}, which is related to $A(T)$ is obtained by multiplying α_{ST} by A_o and I [5], as follows.

$$\alpha_{AT} = A_o I \alpha_{ST}. \quad (6)$$

3.4.2. Limits of Scaling Factors. Scaling performed on the amplitude of real earthquake records should not exceed specific limits. These limits are dependent on the type of problem for which the selection of ground motion is intended for use. In previously conducted studies [3, 19, 23, 44, 45], a scaling constant of 4 is accepted as the upper limit for the analyses of linear elastic structures. However, for the analyses of nonlinear inelastic structures, α_{AT} should be in the range from 0.5 to 2, and for liquefaction, α_{AT} should not be greater than 2.

3.4.3. Criteria for the Selection of Records. In the earthquake codes, it is permissible to use earthquake ground motion records that are artificially generated, previously recorded, or simulated for the linear and nonlinear seismic analysis of buildings and building-type structures within the time domain. However, the earthquake records used should have certain features. For example, the duration of the strong ground motion part of the earthquake record should be no shorter than five times the first natural vibration period of a building not longer than 15 s. In addition, the average of the spectral acceleration records, which is equivalent to the zero period, should be used for earthquake ground motion that is not less than A_{og}. Furthermore, in the earthquake direction considered, the average of the spectral acceleration records that conform to the acceleration record and are used for the 5% damping ratio should not be less than 90% of the elastic spectral acceleration records defined in [35], within a period range between $0.2T_1$ and $2T_1$ with respect to the first (dominant) period T_1. Finally, for linear and nonlinear calculations in the time domain, the maximum of the results, in which three ground motions are used, and the average of results, in which at least seven ground motions are used, is going to be the basis for design.

3.4.4. Method for Selecting and Scaling Real Earthquake Records and Generating Response Spectra. The following records and methods were used in time domain calculations in this study and are summarized as follows:

(1) Data pertaining to the location, ground conditions, history, magnitude, and scaled acceleration value features of records of earthquakes occurring in the CAFZ, as found in the Turkish National Strong Ground Motion Database, are listed in Table 1.

(2) For each N-S (north-south) and E-W (east-west) component, in the period range between $T_S = 0.01$ s and $T_F = 2.00$ s, for a 5% damping ratio, the response spectra were obtained using the Bispec-Earthquake Solutions Programme [46].

(3) The scaling factors for each component of the earthquake records were calculated by matching the response spectra obtained for each earthquake record with the target response spectrum. In this study, the following methods were applied, and they are listed in items 4–7, as follows.

(4) Records with a scaling factor, α_{ST}, greater than 20 and less than 1/20 were eliminated. For example, in Table 1, the scaling factor, α_{ST}, of an earthquake with an epicenter at Sivas-Ulasli (M_L: 3.3) was eliminated for being greater than 20.

Table 3: $S_a^{\text{actual}}(T)$ and $S_a^{\text{target}}(T)$ values.

$T(s)$	$S_a^{\text{actual}}(T)$	$S_a^{\text{target}}(T)$
0.01	0.14	1.10
0.05	0.16	1.51
0.09	0.23	1.91
0.13	0.36	2.32
0.17	0.32	2.50
0.21	0.25	2.50
0.25	0.23	2.50
0.29	0.33	2.50
0.33	0.28	2.50
0.38	0.27	2.50
0.42	0.23	2.42
0.46	0.25	2.25
0.50	0.26	2.10
0.54	0.25	1.97
0.58	0.15	1.86
0.62	0.14	1.76
0.66	0.15	1.68
0.70	0.14	1.60
0.74	0.15	1.53
0.78	0.16	1.46
0.82	0.16	1.40
0.86	0.16	1.35
0.90	0.14	1.30
0.94	0.12	1.26
0.98	0.11	1.22
1.03	0.10	1.18
1.07	0.10	1.14
1.11	0.10	1.11
1.15	0.12	1.08
1.19	0.15	1.05
1.23	0.15	1.02
1.27	0.15	0.99
1.31	0.13	0.97
1.35	0.13	0.94
1.39	0.13	0.92
1.43	0.12	0.90
1.47	0.11	0.88
1.51	0.09	0.86
1.55	0.08	0.84
1.59	0.07	0.83
1.63	0.06	0.81
1.68	0.05	0.79
1.72	0.05	0.78
1.76	0.05	0.77
1.80	0.05	0.75
1.84	0.05	0.74
1.88	0.05	0.73
1.92	0.05	0.71
1.96	0.05	0.70
2.00	0.05	0.69

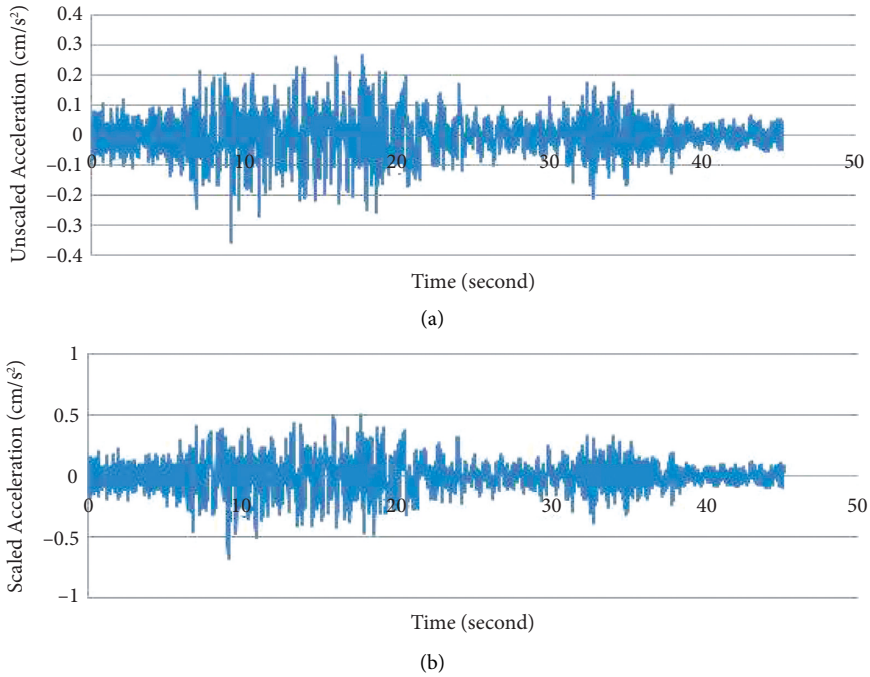

Figure 8: Earthquake with an epicenter at Kayseri-Kocasinan (M_L: 4.8). (a) Unscaled and (b) scaled acceleration record graph of this earthquake in the north-south (N-S) route.

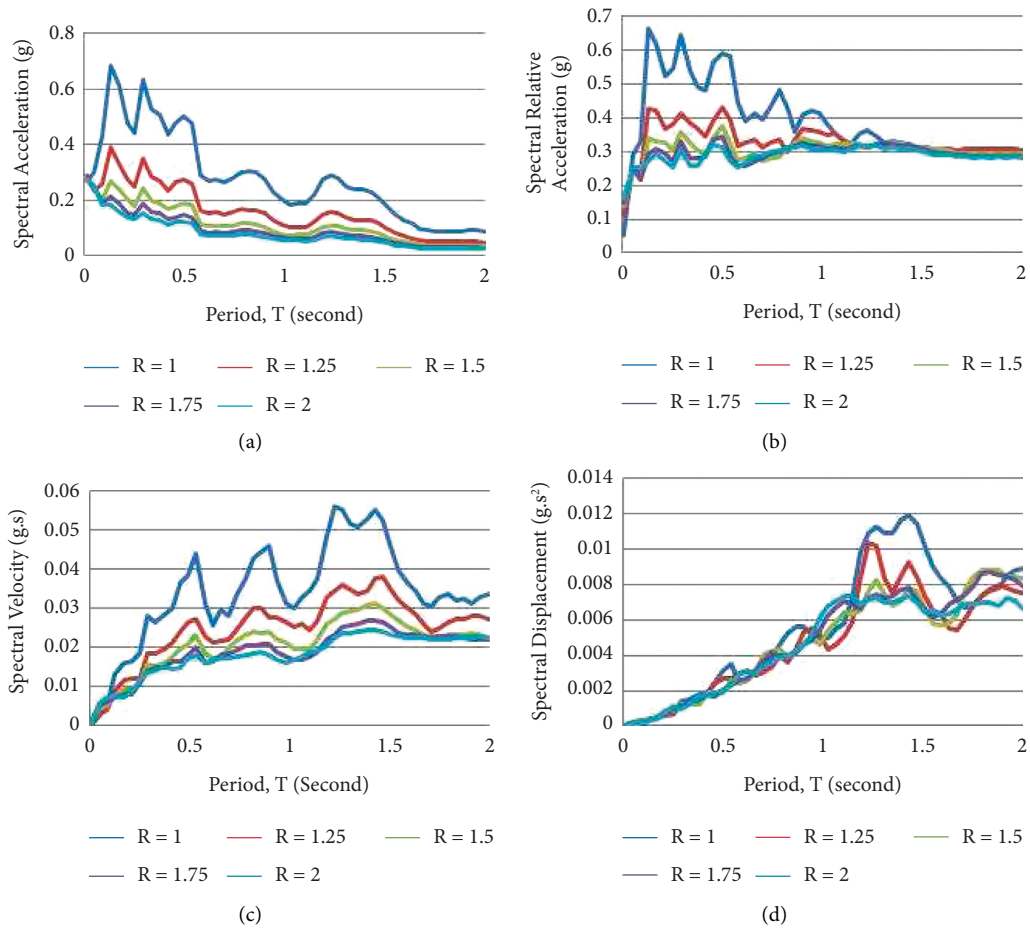

Figure 9: Earthquake with an epicenter at Kayseri-Kocasinan (M_D: 3.7) and the record of north-south (N-S) route. (a) Scaled spectral total acceleration, (b) spectral relative acceleration, (c) spectral velocity, and (d) spectral displacement spectrum graph.

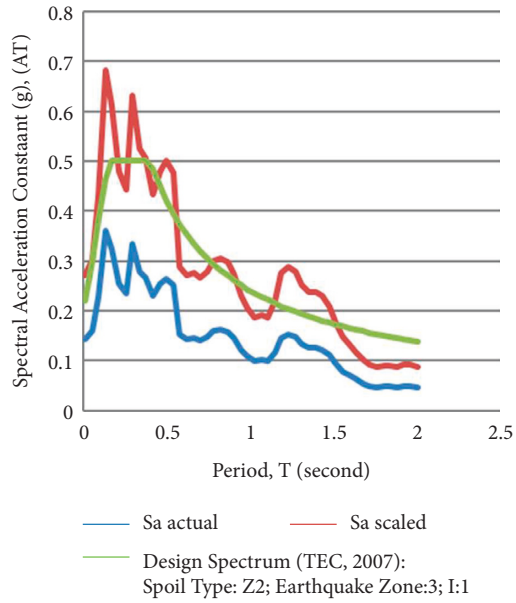

Figure 10: Earthquake with an epicenter at Kayseri-Kocasinan (M_D: 3.7) and response spectrum of north-south (N-S) route record scaled according to elastic design acceleration spectrum.

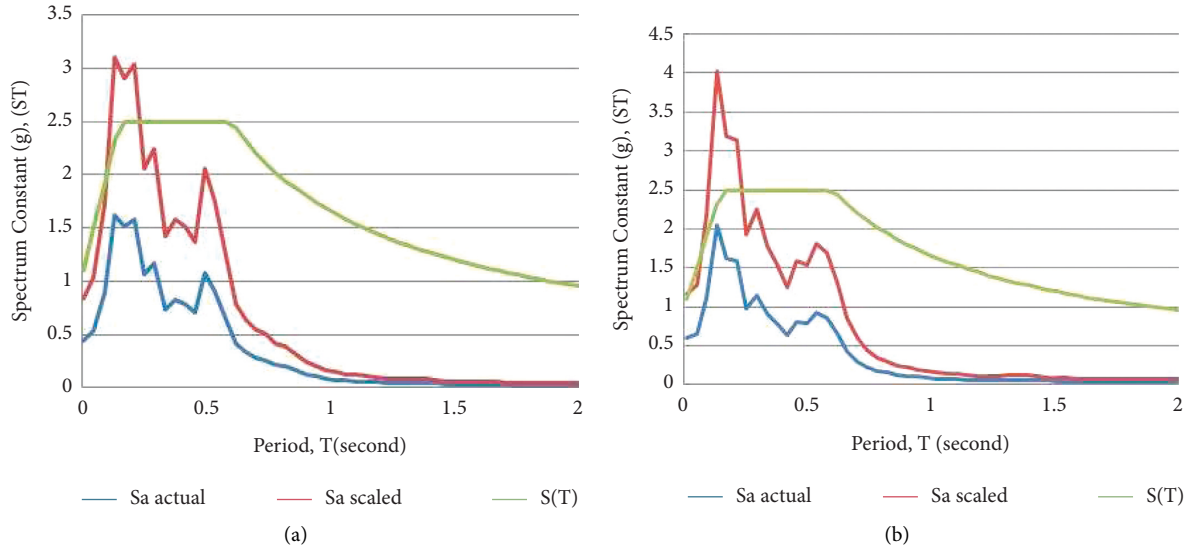

Figure 11: Evaluation of S(T) spectrum constants for (a) North-South (N-S) and (b) East-West (E-W) components of earthquake with epicenter at Sivas (M_D: 4.0).

(5) Scaled response spectrum graphs were created by multiplying data related to real ground motion response spectrum graphs obtained using the Bispec-Earthquake Solutions Programme [46] with the scaling factor, α_{ST}.

(6) The differences between the design spectrum of each component for each record and the response spectrum amplitude of the scaled record, in the period range between $T_S = 0.01$ s and $T_F = 2.00$ s, were computed using the "Sum Relative Errors" formula shown in the following equation.

$$|\text{Sum Relative Error}| = \sum_{TF}^{TS} \left| \left[\frac{\alpha S_a^{\text{actual}}(T) - S_a^{\text{target}}(T)}{S_a^{\text{target}}(T)} \right] \right|. \quad (7)$$

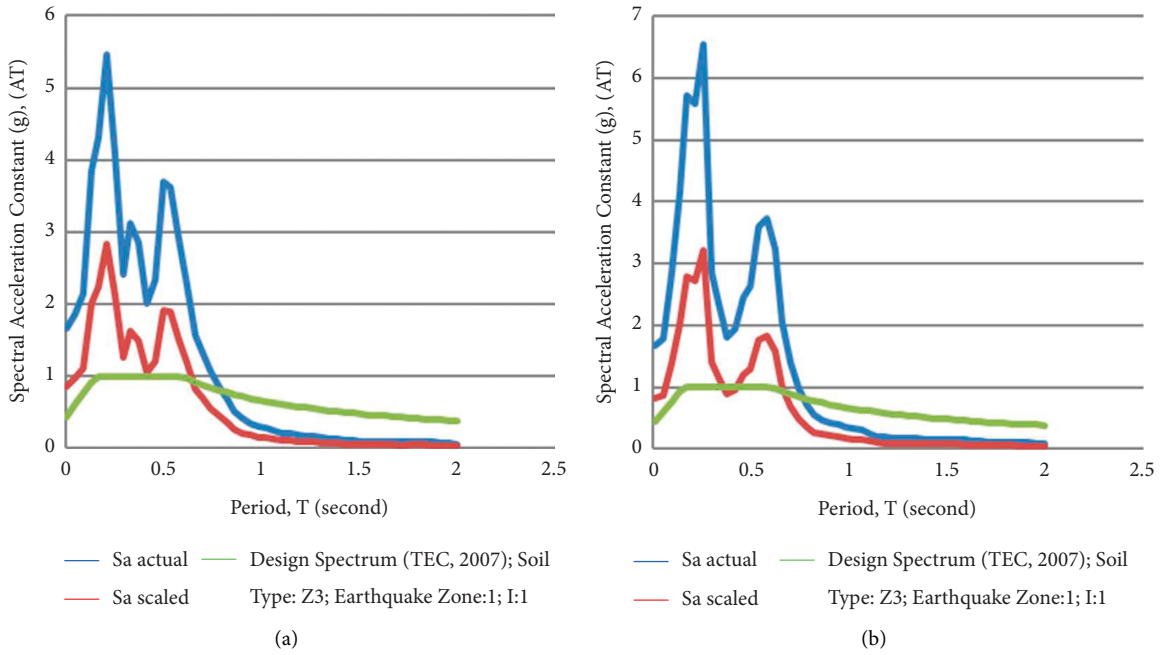

Figure 12: Evaluation of A(T) spectral acceleration constants for (a) North-South (N-S) and (b) East-West (E-W) components of earthquake with epicenter at Sivas (M_D: 4.5).

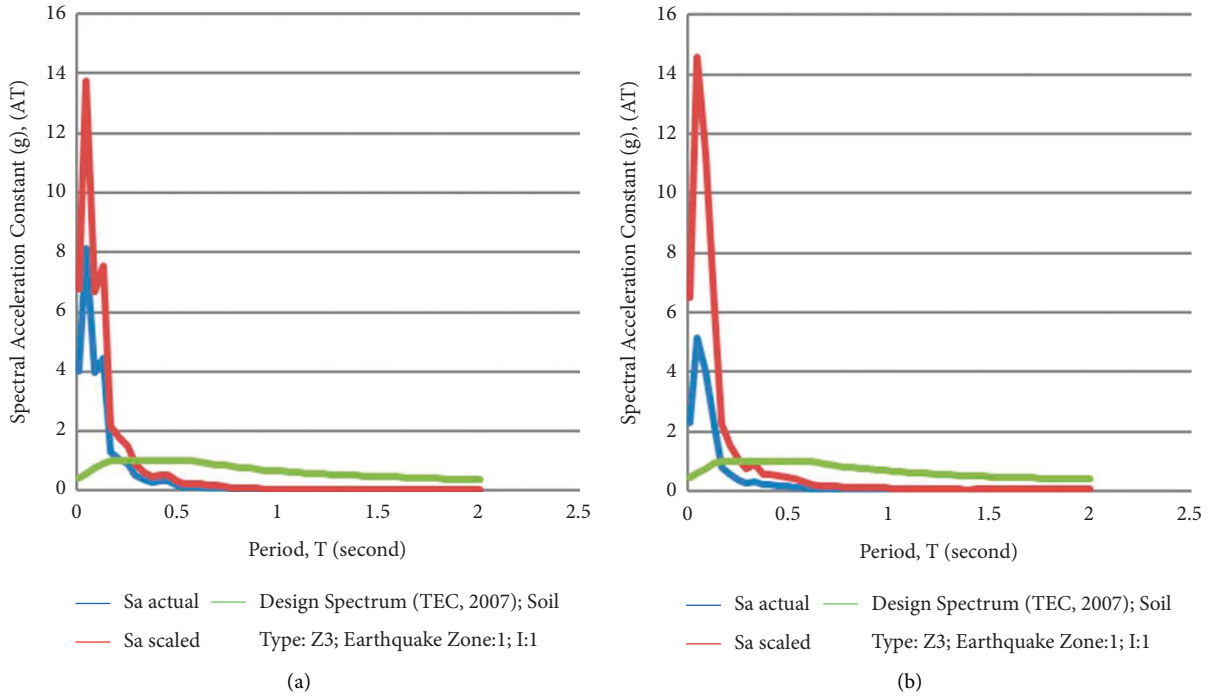

Figure 13: Evaluation of A(T) spectral acceleration constants for (a) North-South (N-S) and (b) East-West (E-W) components of earthquake with epicenter at Sivas (M_D: 2.8).

The error amount is calculated as a percentage by putting the "Sum Relative Error" obtained in the following equation.

$$|\text{Average Relative Error}(\%)| = \frac{1}{k}|\text{Sum Relative Error}| \times 100, \quad (8)$$

where k is the number of period steps (ΔT) used to generate the response spectrum of the record.

$$k = \frac{(T_F - T_S)}{\Delta T}. \quad (9)$$

(7) Each earthquake record was scaled for both the N-S (north-south) and E-W (east-west) components and

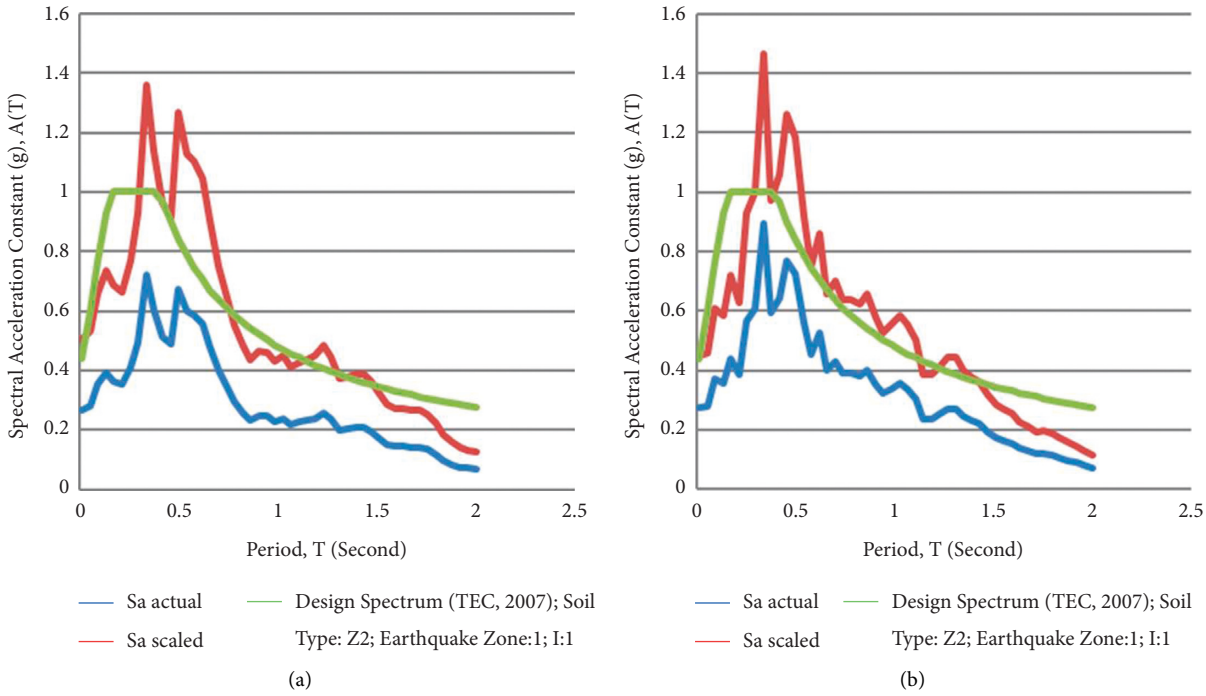

Figure 14: Evaluation of A(T) spectral acceleration constants for (a) North-South (N-S) and (b) East-West (E-W) components of earthquake with epicenter at Kayseri-Kocasinan (M_L: 4.8).

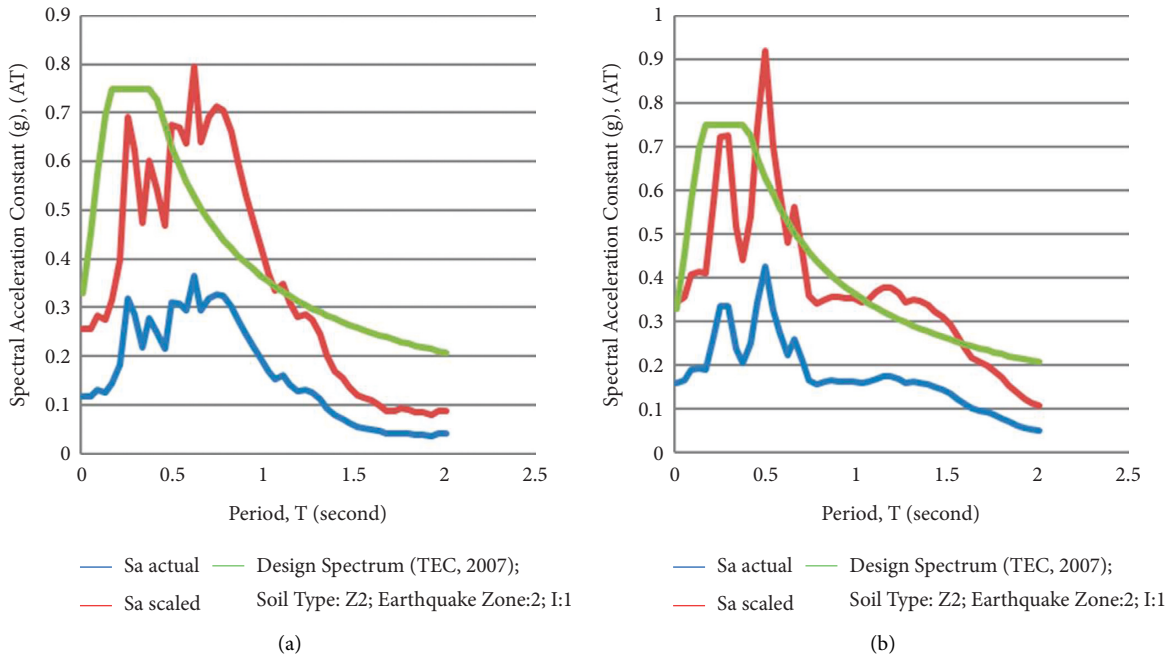

Figure 15: Evaluation of A(T) spectral acceleration constants at Bala station for (a) North-South (N-S) and (b) East-West (E-W) components of earthquake epicenter at Kayseri-Kocasinan (M_L: 4.8).

in the period range between $T_S = 0.01$ s and $T_F = 2.00$ s for the 5% damping ratio obtained. Scaled response spectrum graphs were created using the scaled acceleration record graphs, and the scaled or unscaled response spectrum graphs obtained were then compared to the design acceleration spectra.

Records of earthquakes occurring throughout the CAFZ were grouped as N-S (north-south) and E-W (east-west) according to the characteristics of local soil classes (Z2 and Z3 local site class) at stations where the earthquakes were scaled. The spectrum constant, $S(T)$, which was obtained by scaling to the design acceleration spectra defined, and the

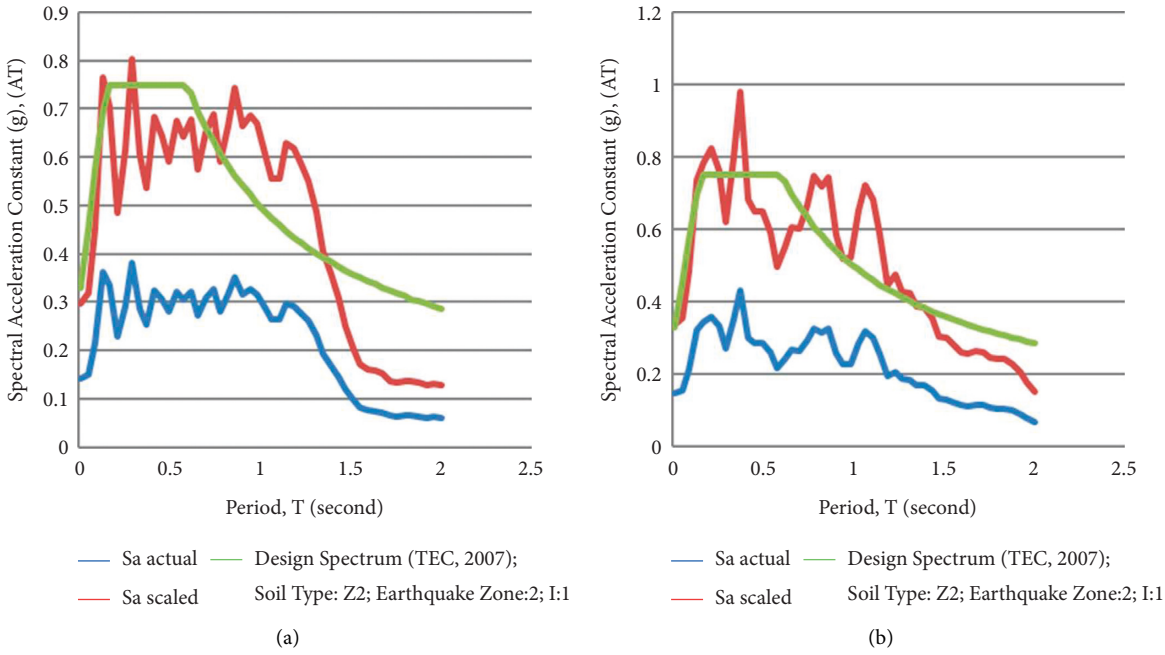

Figure 16: Evaluation of A(T) spectral acceleration constants at S. Kochisar station for (a) North-South (N-S) and (b) East-West (E-W) components of earthquake with epicenter at Kayseri-Kocasinan (M_L: 4.8).

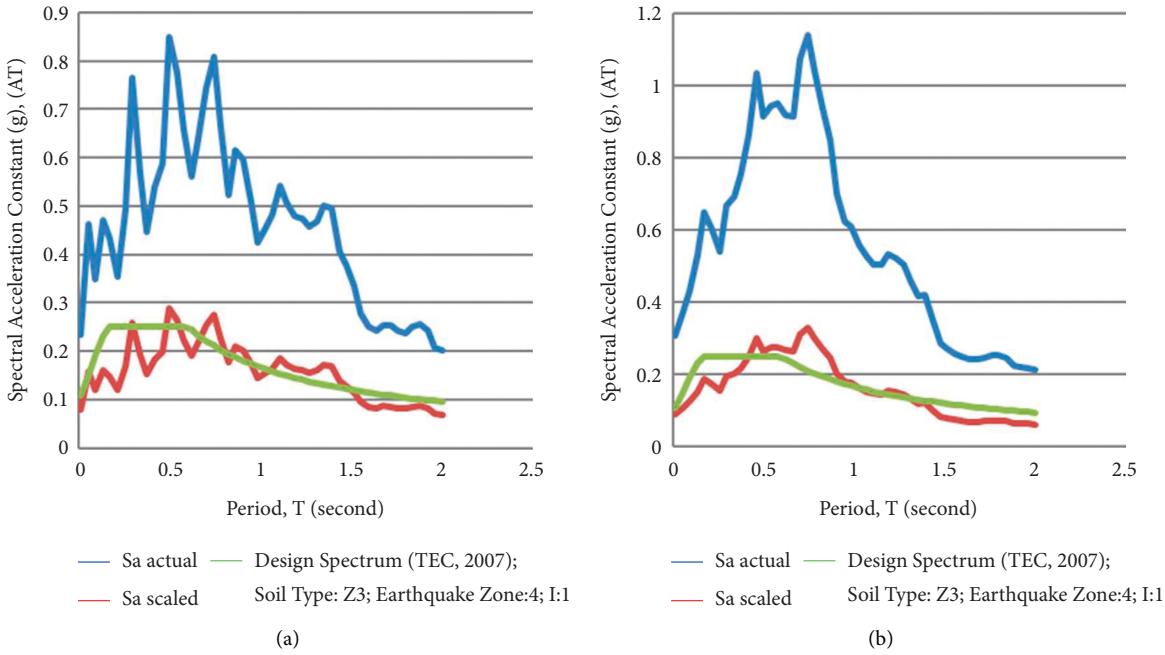

Figure 17: Evaluation of A(T) spectral acceleration constants at Aksaray station for (a) North-South (N-S) and (b) East-West (E-W) components of earthquake with epicenter at Kayseri-Kocasinan (M_L: 4.8).

average spectrum curve obtained using these records is shown in Figures 6 and 7.

3.5. Implementation. In this example, the earthquake record (M_D: 3.7) shown in Table 1 is selected. This event occurred in 2008 along the N-S route at Kayseri-Kocasinan on the CAFZ. The recording station at which the earthquake was scaled is located on a Z2 local site class and in the 3rd degree earthquake zone ($A_o = 0.2$); the building importance factor is selected as $I = 1$.

To enable this record to provide a match with the design acceleration spectrum identified for Z3 local site class, the α_{ST} constant is found to be 8.79 using Equation (3). $S_a^{\text{actual}}(T)$ and $S_a^{\text{target}}(T)$ values used for calculation of α_{ST} are given below in Table 3.

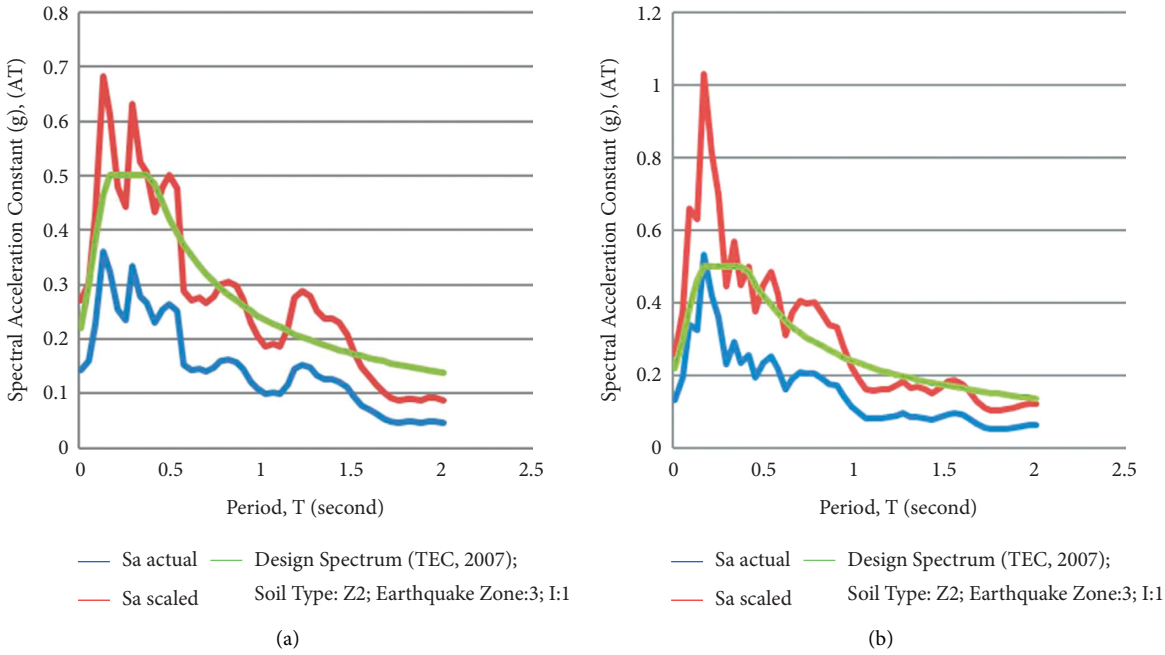

Figure 18: Evaluation of A(T) spectral acceleration constants for (a) North-South (N-S) and (b) East-West (E-W) components of earthquake with epicenter at Kayseri-Kocasinan (M_D: 3.7).

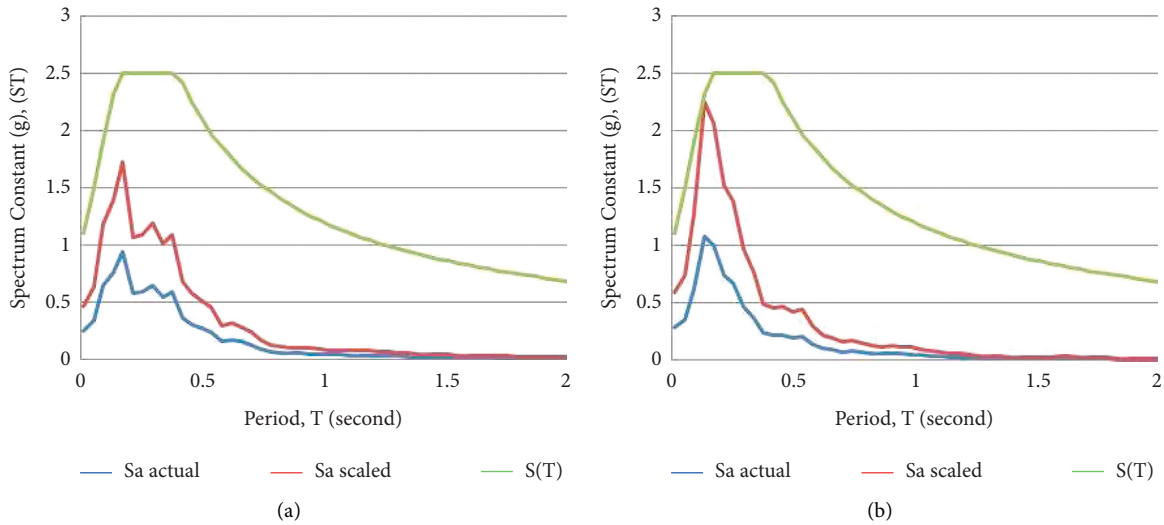

Figure 19: Evaluation of S(T) spectrum constants for (a) North-South (N-S) and (b) East-West (E-W) components of earthquake with epicenter at Kayseri-Kocasinan (M_D: 3.6).

From Equation (3) and Table 3, $\alpha_{ST} = 8.79$ is obtained.

Then, Equation (6) is used to calculate the scaling factor as follows:

$$\alpha_{AT} = A_o I \alpha_{ST} = 0.2 \times 1 \times 8.79 = 1.758. \quad (10)$$

To obtain the scaled record, the amplitudes of earthquake records are thus linearly multiplied by α_{AT}, the scaling constant. Figure 8 shows records that are both scaled and not scaled with α_{AT}; the acceleration response spectra of the scaled records have a period range of between $T_S = 0.01$ s and $T_F = 2$ s. The 5% damping ratio is shown in Figure 9 in the forms of spectral total acceleration, spectral relative acceleration, spectral velocity, and spectral displacement. Figure 10 shows acceleration response spectra with a 5% damping ratio for a SDOF linear system, and a design spectrum for a record scaled with α_{AT} (with respect to this record).

While α_{ST} linear scaling constant is being calculated, it should be considered that the response spectrum that is not scaled in the period range from $T_S = 0.01$ s to $T_F = 2$ s possesses a 5% damping ratio of S_a^{target} E-W (east-west)

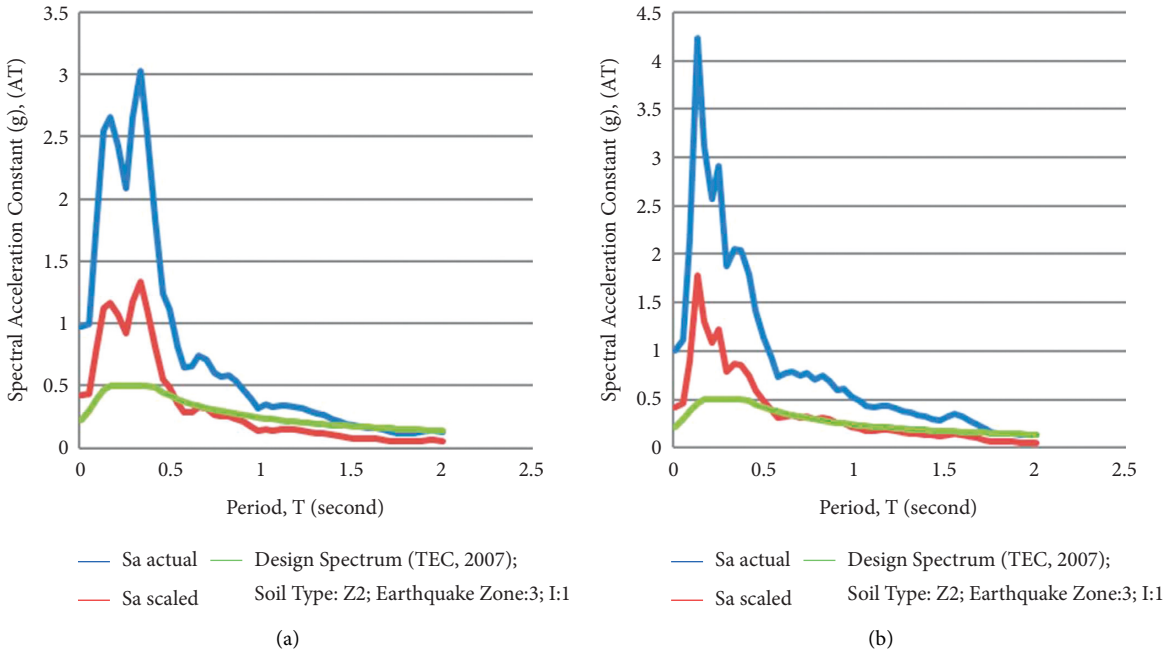

Figure 20: Evaluation of A(T) spectral acceleration constants for (a) North-South (N-S) and (b) East-West (E-W) components of earthquake with epicenter at Kayseri-Kocasinan (M_D: 3.7- M_L: 3.9).

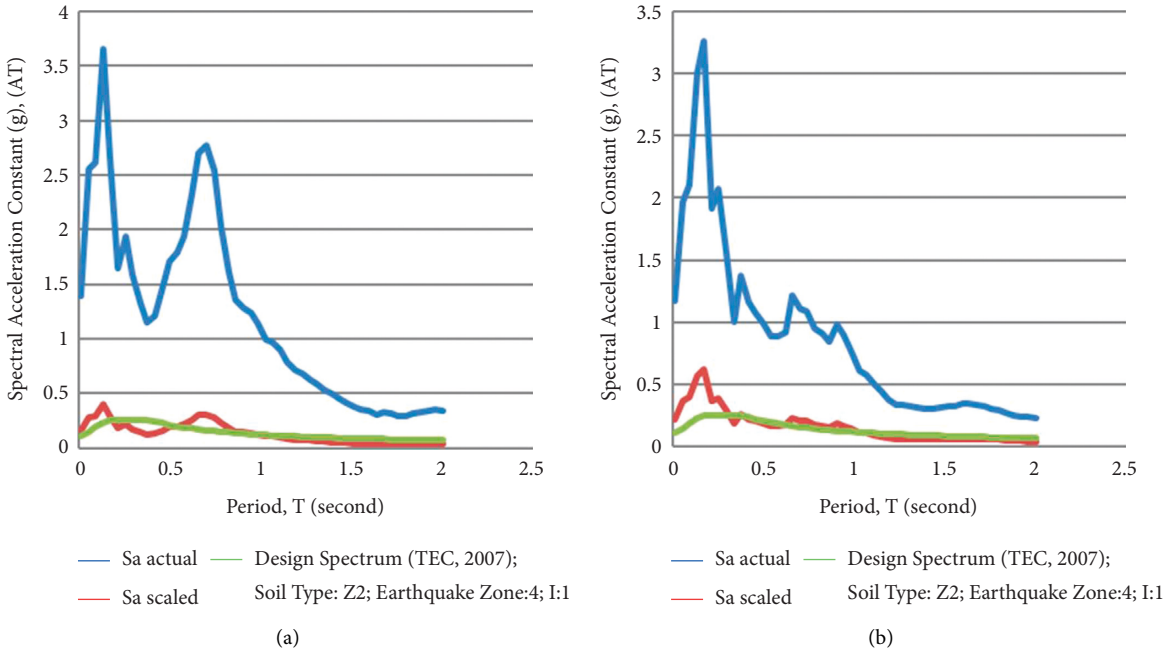

Figure 21: Evaluation of A(T) spectral acceleration constants at Nigde station for (a) North-South (N-S) and (b) East-West (E-W) components of earthquake with epicenter at Nigde-Camardi (M_L: 4.3).

earthquake route record, and for earthquake records measured in local site class Z3 and 3rd earthquake zone, S_a^{target} is the elastic design acceleration spectrum value in Figure 5.

3.6. Scaled Response Spectrum Graphs of Records. Scaled response spectrum graphs of records in the North-South (N-S) and East-West (E-W) earthquake routes that occurred on the CAFZ, according to the elastic design acceleration spectra, are given below in Figures 11–26.

4. Results and Discussion

This is a pioneering study on the analysis of seismic behavior using SDOF systems subjected to ground motions that were recorded in relation to earthquakes occurring on the CAFZ

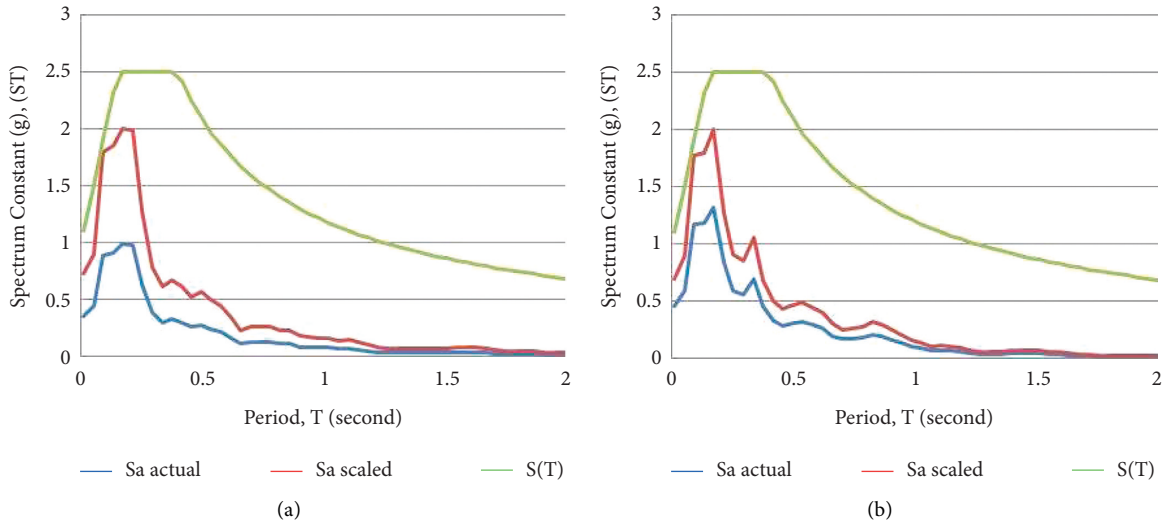

Figure 22: Evaluation of S(T) spectrum constants at Nevsehir station for (a) North-South (N-S) and (b) East-West (E-W) components of earthquake with epicenter at Nigde-Camardi (M_L: 4.3).

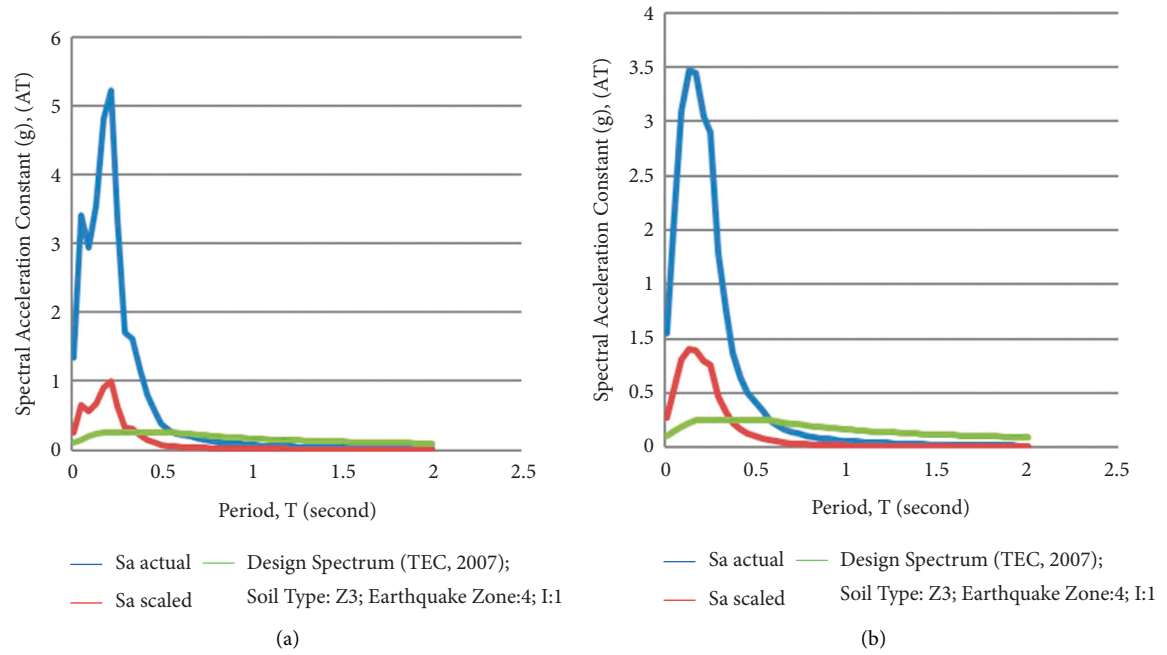

Figure 23: Evaluation of A(T) spectral acceleration constants for (a) North-South (N-S) and (b) East-West (E-W) components of earthquake with epicenter at Nigde-Camardi (M_L: 3.7).

in Turkey. It is considered that the study provides useful results for application in earthquake engineering performance-based design principles within the region.

It is essential that records have particular features for use and that scaling methods are selected to match real ground motion records and design acceleration spectra as defined in [35, 47]. Earthquake ground motion records occurring through this fault zone can then be scaled, thus conforming to the design acceleration spectrum defined.

This study uses the records of 17 ground motions recorded in the Turkish National Strong Ground Motion Database (2015) throughout the fault zone. Table 1 shows the associated station location, ground conditions, distance, magnitude, acceleration values, and scaling factors related to these records. Acceleration record graphs that are both scaled and not scaled for each N-S (north-south) and E-W (east-west) component are shown; and the response spectrum graphs (spectral total acceleration, spectral relative acceleration, spectral velocity, and spectral displacement forms) with a 5% damping ratio of a SDOF linear system within the period range between $T_S = 0.01$ s and $T_F = 2$ s in the time domain are generated using the scaling method.

Compatible records are selected from the 17 ground motion records to fit scaling, with conditions provided in the

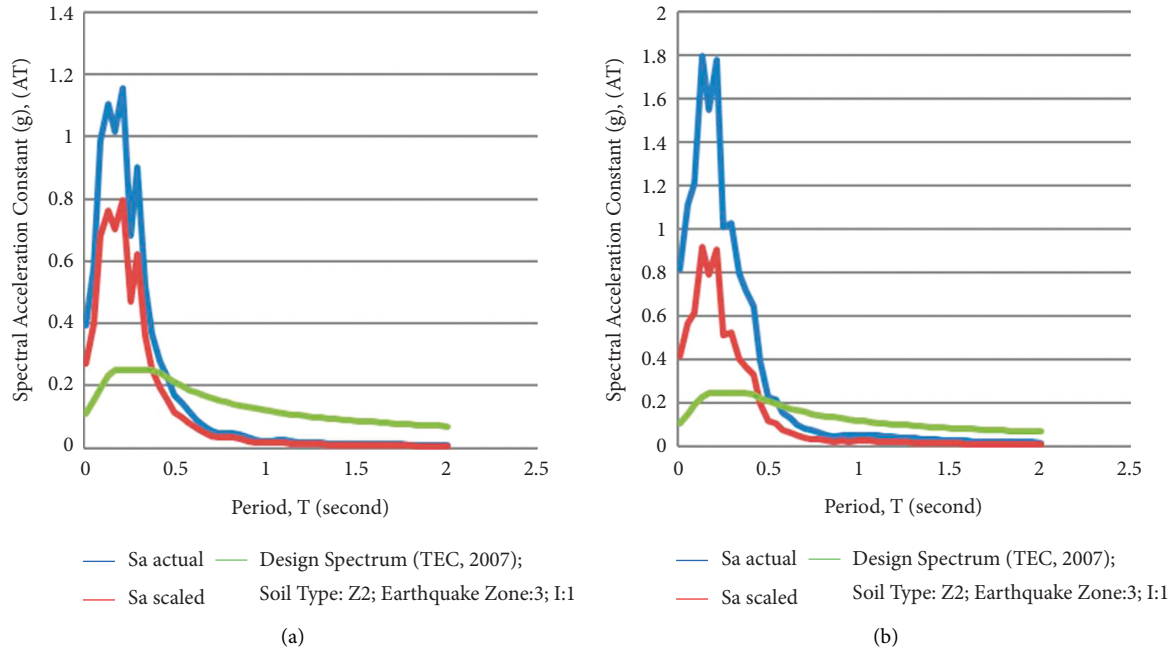

Figure 24: Evaluation of A(T) spectral acceleration constants for (a) North-South (N-S) and (b) East-West (E-W) components of earthquake with epicenter at Sivas-Kangal (M_W: 4.2).

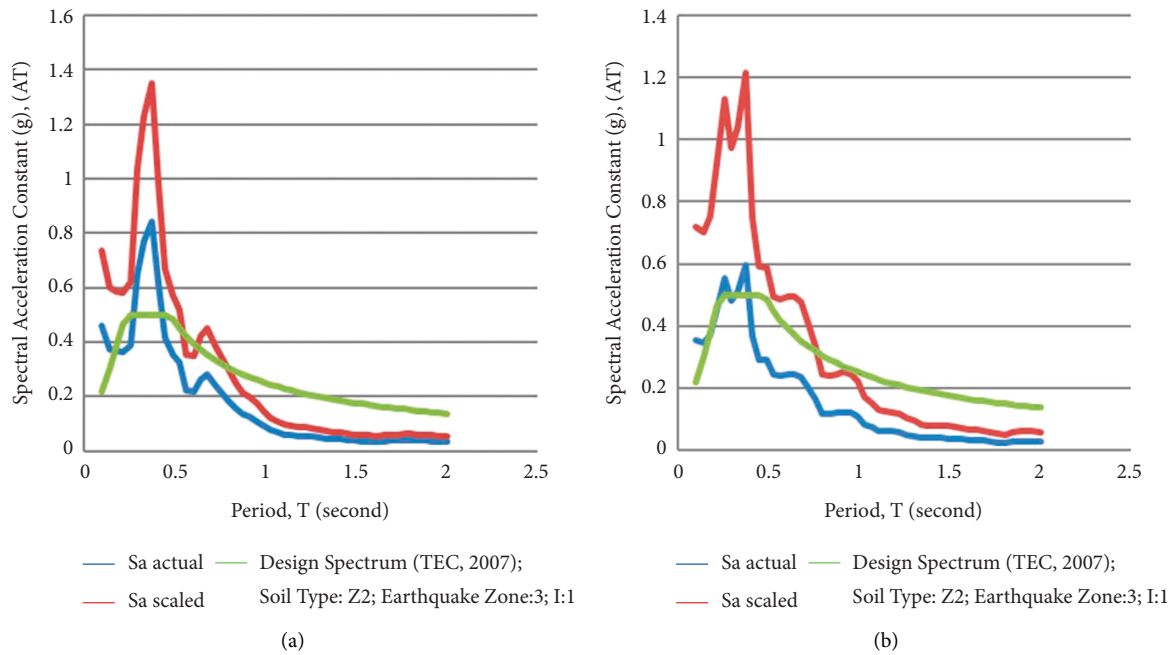

Figure 25: Evaluation of A(T) spectral acceleration constants for (a) North-South (N-S) and (b) East-West (E-W) components of earthquake with epicenter at Kayseri-Kocasinan (M_W: 3.8).

design acceleration spectrum defined. The study then shows the practice of record scaling in the period range between $T_S = 0.01$ s and $T_F = 2$ s with a proper SDOF linear system with a damping ratio of 5%.

The study mentions the importance of the compatible scaling of real earthquake records with the design response spectrum using conditions specified in the earthquake codes. When the earthquakes recorded throughout the CAFZ were examined, some were found to be unsuitable for scaling. By examining response spectra formed by the scaled earthquake records, it was thus possible to understand which earthquake records were suitable or not for scaling in line with the design spectrum.

It should be noted that this is a study based on specific examples of building structures along the CAFZ. Meanwhile, this research method is applicable in other seismic regions of

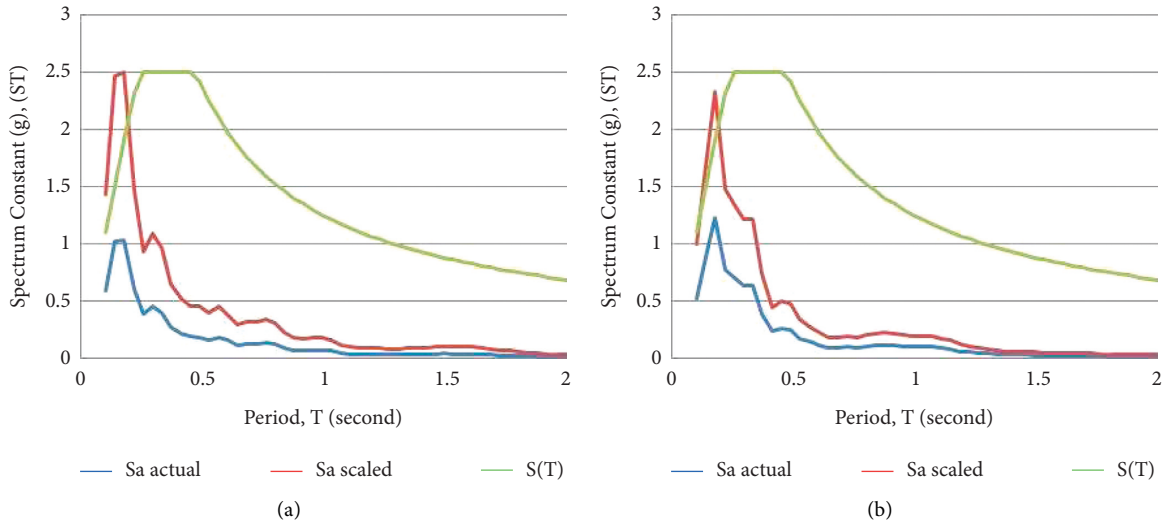

Figure 26: Evaluation of S(T) spectrum constants for (a) North-South (N-S) and (b) East-West (E-W) components of earthquake with epicenter at Sivas-Gemerek (M_W: 3.8).

the world because it is based on current scaling methods available in the literature. This study determines the importance of selecting suitable records with certain features that can be used with the scaling method to ensure that real ground motion records match the design acceleration spectrum defined in the earthquake codes.

Data Availability

The data used to support the findings of the study can be obtained from the corresponding author upon request.

Disclosure

This research was performed as part of the M. Sc. Thesis of Mr. Erhan Gumus at Nigde Omer Halisdemir University, Turkey.

Conflicts of Interest

The authors declare that they have no conflicts of interest regarding the publication of this paper.

References

[1] N. A. Abrahamson, "Non-stationary spectral matching Program," RSPMATCH, User's Manual, 1993.

[2] D. M. Boore, "Simulation of ground motion using the Stochastic method," *Pure and Applied Geophysics*, vol. 160, no. 3, pp. 635–676, 2003.

[3] J. J. Bommer and A. B. Acevedo, "The Use of real earthquake accelerograms as input to dynamic analysis," *Journal of Earthquake Engineering*, vol. 8, no. sup001, pp. 43–91, 2004.

[4] J. J. Bommer, A. B. Acevedo, and J. Douglas, "The selection and scaling of real earthquake accelerograms for Use in seismic design and assessment," *Proceedings of ACI International Conference on Seismic Bridge Design and Retrofit*, American Concrete Institute, 2003.

[5] Y. M. Fahjan, "Selection and scaling of real earthquake accelerograms to fit the Turkish design spectra (DBYBHY, 2007)," *Chamber of Civil Engineers Technical Journal*, pp. 4423–4444, 2008.

[6] M. M. Hachem, N. J. Mathias, Y. Y. Wang et al., "An International Comparison of ground motion selection criteria for seismic design," in *Proceedings of the Joint IABSE–fib Conference*, Dubrovnik, Croatia, May 2010.

[7] A. Akinci, L. Malagnini, R. B. Herrmann, R. Gok, and M. B. Sørensen, "Ground motion scaling in the Marmara region, Turkey," *Geophysical Journal International*, vol. 166, no. 2, pp. 635–651, 2006.

[8] P. Bodin, L. Malagnini, and A. Akinci, "Ground-motion scaling in the Kachchh basin, India, Deduced from Aftershocks of the 2001 Mw 7.6 Bhuj earthquake," *Bulletin of the Seismological Society of America*, vol. 94, no. 5, pp. 1658–1669, 2004.

[9] L. C. Haar, J. B. Fletcher, and C. S. Mueller, "The 1982 Enola, Arkansas, swarm and scaling of ground motion in the eastern United States," *Bulletin of the Seismological Society of America*, vol. 74, no. 6, pp. 2463–2482, 1984.

[10] I. Iervolino, E. Cosenza, and C. Galasso, "Shedding some Light on seismic input selection in Eurocode 8," in *Proceedings of the Eurocode 8 Perspectives from the Italian Standpoint Workshop*, pp. 3–12, Doppiavoce, Naples, Italy, 2009.

[11] A. H. Kayhan, "Obtaining the unscaled accelerogram setting compatible with Eurocode-8 by Armony research technic," in *Proceedings of the Turkish Earthquake Engineering and Seismology Conference*, METU, Ankara, Turkey, October 2011.

[12] L. Malagnini, R. B. Herrmann, and K. Koch, "Regional ground-motion scaling in Central Europe," *Bulletin of the Seismological Society of America*, vol. 90, no. 4, pp. 1052–1061, 2000.

[13] L. Malagnini, R. B. Herrmann, and M. Di Bona, "Ground-motion scaling in the Apennines (Italy)," *Bulletin of the Seismological Society of America*, vol. 90, no. 4, pp. 1062–1081, 2000.

[14] P. Morasca, L. Malagnini, A. Akinci, D. Spallarossa, and R. B. Herrmann, "Ground-motion scaling in the western Alps," *Journal of Seismology*, vol. 10, no. 3, pp. 315–333, 2006.

[15] A. Rovelli, O. Bonamassa, M. Cocco, M. Di Bona, and S. Mazza, "Scaling laws and spectral parameters of the ground motion in active extensional areas in Italy," *Bulletin of the*

Seismological Society of America, vol. 78, no. 2, pp. 530–560, 1988.

[16] L. Scognamiglio, L. Malagnini, and A. Akinci, "Ground-motion scaling in eastern Sicily, Italy," *Bulletin of the Seismological Society of America*, vol. 95, no. 2, pp. 568–578, 2005.

[17] J. P. Stewart, S. Midorikawa, R. W. Graves et al., "Implications of the Mw9.0 Tohoku-Oki earthquake for ground motion scaling with source, Path, and site parameters," *Earthquake Spectra*, vol. 29, no. 1_suppl, pp. 1–21, 2013.

[18] C. H. Scholz, "Scaling relations for strong ground motion in large earthquakes," *Bulletin of the Seismological Society of America*, vol. 72, no. 6A, pp. 1903–1909, 1982.

[19] A. McGarr, "Scaling of ground motion parameters, state of stress, and focal depth," *Journal of Geophysical Research: Solid Earth*, vol. 89, no. B8, pp. 6969–6979, 1984.

[20] P. G. Somerville, "Magnitude scaling of near fault ground motions," *Earthquake Engineering and Engineering Seismology*, vol. 2, no. 2, pp. 15–24, 2000.

[21] Y. C. Kurama and K. T. Farrow, "Ground motion scaling methods for different site conditions and structure characteristics," *Earthquake Engineering & Structural Dynamics*, vol. 32, no. 15, pp. 2425–2450, 2003.

[22] F. Naeim, A. Alimoradi, and S. Pezeshk, "Selection and scaling of ground motion time histories for structural design using genetic algorithms," *Earthquake Spectra*, vol. 20, no. 2, pp. 413–426, 2004.

[23] J. Watson-Lamprey and N. Abrahamson, "Selection of ground motion time series and limits on scaling," *Soil Dynamics and Earthquake Engineering*, vol. 26, no. 5, pp. 477–482, 2006.

[24] N. Luco and P. Bazzurro, "Does amplitude scaling of ground motion records result in biased nonlinear structural drift responses?" *Earthquake Engineering & Structural Dynamics*, vol. 36, no. 13, pp. 1813–1835, 2007.

[25] A. Kottke and E. M. Rathje, "A semi-automated procedure for selecting and scaling recorded earthquake motions for dynamic analysis," *Earthquake Spectra*, vol. 24, no. 4, pp. 911–932, 2008.

[26] Y. N. Huang, A. S. Whittaker, N. Luco, and R. O. Hamburger, "Scaling earthquake ground motions for performance-based assessment of buildings," *Journal of Structural Engineering*, vol. 137, no. 3, pp. 311–321, 2011.

[27] E. I. Katsanos, A. G. Sextos, and G. D. Manolis, "Selection of earthquake ground motion records: a state-of-the-art review from a structural engineering perspective," *Soil Dynamics and Earthquake Engineering*, vol. 30, no. 4, pp. 157–169, 2010.

[28] N. Jayaram, T. Lin, and J. W. Baker, "A computationally efficient ground-motion selection algorithm for matching a target response spectrum mean and variance," *Earthquake Spectra*, vol. 27, no. 3, pp. 797–815, 2011.

[29] I. Takewaki and H. Tsujimoto, "Scaling of design earthquake ground motions for tall buildings based on drift and input energy demands," *Earthquakes and Structures*, vol. 2, no. 2, pp. 171–187, 2011.

[30] B. O. Ay and S. Akkar, "A procedure on ground motion selection and scaling for nonlinear response of simple structural systems," *Earthquake Engineering & Structural Dynamics*, vol. 41, no. 12, pp. 1693–1707, 2012.

[31] C. B. Haselton, A. S. Whittaker, A. Hortacsu, J. W. Baker, J. Bray, and D. N. Grant, "Selecting and scaling earthquake ground motions for performing response-history analyses," in *Proceedings of the 15th World Conference on Earthquake Engineering*, Lisbon, Portugal, November 2012.

[32] L. Al Atik, A. Kottke, N. Abrahamson, and J. Hollenback, "Kappa (K) scaling of ground motion prediction equations using an Inverse random vibration theory approach," *Bulletin of the Seismological Society of America*, vol. 104, no. 1, pp. 336–346, 2014.

[33] N. N. Ambraseys and C. Finkel, *The Seismicity of Turkey and adjacent areas*, p. 240, UNESCO, Istanbul, 1995.

[34] N. Pinar and E. Lahn, *Turkish Earthquake Catalog with Descriptions*, Turkey Ministry of Public Works and Settlement, The General Directorate of Construction Affairs, Serial 6, Technical Report 36, p. 153, 1952.

[35] Turkish Earthquake Code (Tec), *Specification for Buildings to Be Built in Seismic Zones*, Ministry of Public Works and Settlement, Government of the Republic of Turkey, Ankara, Turkey, 2007.

[36] C. Yetis, *Geology Analysis of Near and Distant Region of Camardi (Nigde) and Characteristics of the Ecemis Fault Zone between Maden Strait and Kamisli*, PhD Thesis, p. 164, Istanbul University, Faculty of Sciences, Istanbul, Turkey, 1978.

[37] C. Yetis, "Geology of the Camardi (Nigde) region and the characteristics of the Ecemis fault zone between maden Bogazi and Kamisli," *Revue de la Faculte des Scienses*, vol. 43, pp. 41–61, 1978.

[38] A. Kocyigit and A. A. Ozacar, "Extensional neotectonic Regime through the NE Edge of the outer Isparta angle, SW Turkey: new field and seismic data," *Turkish Journal of Earth Sciences*, vol. 12, pp. 67–90, 2003.

[39] E. Bozkurt, "Neotectonics of Turkey – a synthesis," *Geodinamica Acta*, vol. 14, no. 1-3, pp. 3–30, 2001.

[40] Kyhdata, "Strong ground motion Database of Turkey (SGMDT)," 2015, http://kyhdata.deprem.gov.tr.

[41] J. P. Stewart, S. J. Chiou, J. D. Bray, R. W. Graves, P. G. Somerville, and N. A. Abrahamson, *Ground Motion Evaluation Procedures for Performance-Based Design*, PEER Report 2001/09, Pacific Earthquake Engineering Research Center, University of California, Berkeley, USA, 2001.

[42] A. S. Nikolaou, *A GIS Platform for Earthquake Risk Analysis*, Ph.D. Dissertation, State University of New York at Buffalo, USA, 1998.

[43] Z. Ozdemir and Y. M. Fahjan, "Comparison of scaling methods of real earthquake records conforming to design spectrum in time and frequency domain," in *Proceedings of the 6th National Earthquake Engineering Conference*, Istanbul, Turkey, October 2007.

[44] E. L. Krinitzsky and F. K. Chang, *Specifying Peak Motions for Design Earthquakes, State-Of The-Art for Assessing Earthquake Hazards in the United States*, Report 7, Miscellaneous Paper S-73-1, US Army Corps of Engineers, USA, 1977.

[45] E. H. Vanmarcke, *State-of-the-Art for Assessing Earthquake Hazards in the United States: Representation of Earthquake Ground Motions – Scaled Accelerograms and Equivalent Response Spectra*, Miscellaneous Paper S-73-1, Report 14, Vicksburg, US Army Corps of Engineers Waterways Experiment Station, Mississippi, USA, 1979.

[46] M. Hachem, "Bispec-earthquake Solutions Programme," Bispec Version 2.20, 2015.

[47] Turkish Building Earthquake Code (Tbec), *Specification for Buildings to Be Built in Seismic Zones, Disaster and Emergency Management Presidency*, Government of Republic of Turkey, Ankara, Turkey, 2018.